IEEE Access
Multidisciplinary | Rapid Review | Open Access Journal

SPECIAL SECTION ON ADVANCED BIG DATA ANALYSIS FOR VEHICULAR SOCIAL NETWORKS

Received December 20, 2018, accepted December 29, 2018, date of publication January 3, 2019, date of current version January 23, 2019.

Digital Object Identifier 10.1109/ACCESS.2019.2890819

A Data-Driven-Based Wavelet Support Vector Approach for Passenger Flow Forecasting of the Metropolitan Hub

MING TANG[1,2], ZHIWU LI[3,4], (Fellow, IEEE), AND GUANGDONG TIAN[1,5], (Member, IEEE)

[1]Transportation College, Jilin University, Changchun 130022, China
[2]School of Management, Jilin University, Changchun 130022, China
[3]Institute of Systems Engineering, Macau University of Science and Technology, Macau 999078, China
[4]School of Electro-Mechanical Engineering, Xidian University, Xi'an 710071, China
[5]School of Mechanical Engineering, Shandong University, Jinan 250061, China

Corresponding author: Guangdong Tian (tiangd2013@163.com)

This work was supported in part by the National Natural Science Foundation of China under Grant 51775238 and in part by the Funds for International Cooperation and Exchange of the National Natural Science Foundation of China under Grant 51561125002.

ABSTRACT With the rapid development of the construction and operation of mass transit hubs, passenger data collection, modeling, and prediction for optimal control have become very important. In this paper, pedestrian facilities are abstracted into connected nodes, and the passenger flow network is formed according to the facility connection relationship determined by the traffic organization; therefore, the state variables of the hub, such as saturation, and the traveling time can be estimated by pedestrian flow information collected by camera monitors and a free Wi-Fi network, including the fast analysis of data features and traffic flow prediction. The method is applied to a real case. The features of pedestrian flows are classified as chaotic and nonchaotic. We use a regression model to predict the nonchaotic situation, and the wavelet support vector machine model is proposed for the chaotic. The results can be used for the control of exits and ramps in the hub.

INDEX TERMS Transit hub, streamline network, chaos, wavelet support vector, data-driven.

I. INTRODUCTION

With the rapid development of social economy and increasing traffic congestion, public transportation and slow traffic are increasingly valued by researchers. As an important link of various modes of transportation, urban transit hubs directly affect the attractiveness of public traffic modes to travelers and the smoothness of the entire urban transport network. We abstract the urban transit hub facility layout and pedestrian streamline organization into a pedestrian streamline network [1], [2], in which facilities such as the ticket gate, wicket and passageway are abstracted into adjustable nodes. Passenger flow demand information and hub operation status information are integrated, aiming at the efficient use of the hub system transfer function under the premises of travel safety and comfort.

The passenger flows are the input and output of pedestrian facilities. This information can be observed from video, cell phone signals and other modern data acquisition methods. The saturation of the facilities and travel time of the passengers can be estimated based on these online data and perdition data, and the estimation can be used for the coordination control of the passenger flow and pedestrian facilities. Thus, passenger flow forecasting was the core component of the management and control system in the comprehensive passenger transport hub and the precondition of the traffic control and guidance, because the forecasting methods can provide the future states of the system for proactive management and traveler information service. The method of short-term traffic flow forecasting falls into two categories. The first is the time series method, based on historical section data of traffic flow, and the second is the filtering and estimating method, based on the section data of upstream traffic flow. Most methods were developed for the prediction of vehicle traffic flow [3]–[9], [33]–[35].

In this work, we focus on the first type of method, the traffic flow time series method. Based on the reconstruction phase space method and the analysis of Lyapunov exponents, Sun *et al.* [8] and Guo *et al.* [9] found that most traffic flows have a fractal character in a certain scale range. References [10]–[14] showed that the chaotic time series

forecasting method has better prediction accuracy based on reconstruction of the phase space technique. The method of support vector machines (SVM) uses machine learning based on the statistical learning theory and has been widely applied in the fields of classification and regression including traffic flow prediction [17]–[19]. Furthermore, the kernel of an SVM can be alternated with a wavelet function that satisfies the admissible condition [20], [21], so the wavelet support vector machine (WSVM) was created. The WSVM method has been widely used in many engineering fields with satisfactory results [22]–[25], [30]–[32]. The chaotic characteristics of pedestrian flows at various pedestrian facilities remained unknown, and exploration of the WSVM method for time series of pedestrian flow prediction was valuable for achieving greater prediction accuracy [33]–[36].

In this manuscript, the pedestrian flow data were collected from a comprehensive passenger transport hub in Beijing. We investigated the chaotic characteristics of the pedestrian flow by reconstructing phase space techniques and constructing the chaotic wavelet support vector regression model for pedestrian flow forecasting. The contributions of our work were the following: (1) pedestrians flows at various facilities in the hub have chaotic characteristics except at the escalators, because the pedestrians move at the same speed; (2) the WSVM model for short-term pedestrian flow forecasting was proposed based on the reconstructed phase space.

The rest of this paper is organized as follows: Section II analyzes the chaotic characteristics of short-term pedestrian flow. Section III constructs the chaotic wavelet support machine model for pedestrian flow forecasting. Section IV is an application using real data collected from a passenger transport hub. Finally, Section V concludes our work and describes some future research issues.

II. THE PASSENGER FLOW NETWORK MODEL

There are many passenger facilities in a mass transit hub. The topology of these facilities is restricted to their relative positions and the traffic organization of the hub. In the network, each facility is abstracted as a point, and the link between two points represents the interface of the points (namely, two connected facilities).

Each point (trait point) in the network represents a passenger facility and is set as an object with attributes of geometry and status. The status is described by variables of saturation, travel time, etc. In Fig. 1, we can directly observe the status of "entrance," "Stair1," and "Stair2" by a camera monitor, but the status of "hall" is not observed because of its large area. However, we can estimate the status of "hall" (the green point in Fig. 1 (a)) by observing and predicting the flows of the interfaces between "hall" and its connected facilities. This can be described by the formula

$$\begin{aligned} Q(t) &= Q(t-1) + f1 - (f2 + f3), \\ S(t) &= Q(t)/Q_{Max}, \end{aligned} \tag{1}$$

where $Q(t)$ is the number of passengers in the facility at time step t; $f1, f2$ and $f3$ denote the flows of the links (see Fig. 1);

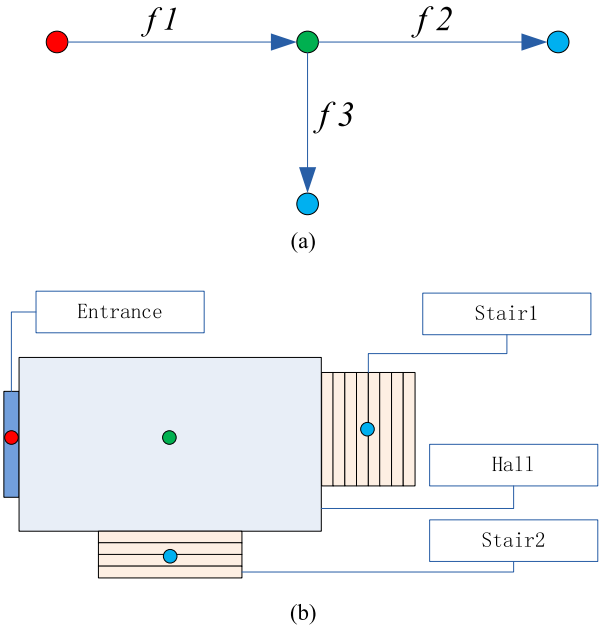

FIGURE 1. Schematic diagram of the passenger flow network and facilities in a mass transit hub. (a) Passenger flow network. (b) Layout of facilities.

and $S(t)$ denotes the saturation of the facility at time step t. Based on equation (1), the in-flow $f1$, and the out-flow $(f2 + f3)$, we can estimate the variable values of the facility status.

III. ANALYSIS OF CHAOTIC CHARACTERISTICS OF PEDESTRIAN FLOWS

In this section, we discuss the chaotic characteristics of in-flow and out-flow of the facilities in a mass transit hub.

A. PHASE SPACE RECONSTRUCTION

For a one-dimensional time series, the chaotic attractor can be reconstructed, and the embedding dimension m and delay time τ should be determined for its reconstruction.

Suppose that the length of a pedestrian flow time series $x(t)$ is n, where the value time step t is set from 1 to n. Let the embedding dimension be m and delay time be τ; the reconstruction phase space R^m can be described as follows:

$$Y(t) = (x(t), x(t+\tau), ..., x(t+(m-1)\tau)), \tag{2}$$

where time step $t = 1, 2, ..., n$. Delay time τ is determined by the autocorrelation function

$$C(\tau) = \sum_{t}^{n-\tau} (x(t) - \bar{x})(x(t+\tau) - \bar{x}) \Big/ \sum_{t}^{n} (x(t) - \bar{x})^2, \tag{3}$$

where the value of delay time τ can be determined by an empirical method whose value is satisfied by $C(\tau) = (1 - 1/e) \cdot C(1)$. The embedding dimension can be determined by the method of pseudo neighbor points, in which some nonneighbor points change into pseudo neighbor points when the value of embedding dimension m is too small. Tracking the number of pairs of pseudo neighbor points, when the

number of pairs does not increase with increasing value of embedding dimension m, the phase space is considered to be expanded completely. The corresponding algorithm for finding pseudo neighbor points is described in Algorithm 1.

Algorithm 1 Finding Pseudo Neighbor Points

Step 1 The time series is $x(t)$, and the time delay is τ; set the initial value of embedding dimension $m = 1$;

Step 2 Reconstruct the phase space based on the series $x(t)$, τ and m; loop the phase points, find their nearest neighbors, and calculate their distance;

Step 3 Calculate criterion 1 and criterion 2,

$$|x(i+m\tau) - x(j+m\tau)| \Big/ \left\|X_i - X_j\right\| > L1, \tag{4}$$

$$\left((x(i+m\tau) - x(j+m\tau))^2 + \left\|X_i - X_j\right\|\right)^{1/2} \cdot \left(n^{-1}\sum_{k=1}^{n}(x(k) - \bar{x})^2\right)^{-1} > L2 \tag{5}$$

where phase point $X_i = (x(i), x(i+\tau), ..., x(i+(m-1)\tau))$, and $\bar{x}$ is the mean value of time series $x(t)$. If a phase point is satisfied by one of the two criteria, the point is labeled as the pseudo neighbor point;

Step 4 Calculate the number of pseudo neighbor points. If the number does not decrease with increasing embedding dimension m, the algorithm ends; otherwise, set $m = (m+1)$ and jump to Step 2.

B. THE LYAPUNOV EXPONENT

In one-dimensional dynamical system $x_{n+1} = F(x_n)$, the variation of distance between two neighbor points in the next time step depends on the value of derivative dF/dx. If the number of iterations is N, let the initial distance between two neighbor points be ε, and $\lambda = mean(Ln(dF/dx))$, so the distance after N iterations will be as follows:

$$\left\|F^n(x_0+\varepsilon) - F^n(x_0)\right\| = \varepsilon e^{n\lambda(x_0)}, \tag{6}$$

Let the variables $\varepsilon \to \infty, N \to \infty$; we can then obtain the equation

$$\lambda = \lim_{N\to\infty}\frac{1}{N}\sum_{i=0}^{N-1} Ln\left|dF^i/dx\right|_{x=x_0}, \tag{7}$$

where λ in the Lyapunov exponent of the dynamical system, which describes the separation velocity between the neighbor points of the phase space in each time step. For the reconstruction phase space of time series, the largest Lyapunov exponent was calculate using Algorithm 2.

C. KOLMOGOROV ENTROPY AND CORRELATION DIMENSION

Local instability of chaotic trajectories leads to separation of adjacent orbits at exponential rates. Kolmogorov entropy (K-Entropy) is a measure for describing the separation speed of adjacent orbits, and the reciprocal of K-Entropy is an index

Algorithm 2 Calculation of Largest Lyapunov Exponent

Step 1 Set initial phase point $Y(t_1)$, find the nearest neighbor point $Y(t_j)$ of $Y(t_0)$, and set $L_1 = \left\|Y(t_1) - Y(t_j)\right\|$;

Step 2 Track the variation of the distance L_1 with the time step accumulation; at time t_2 and $L_1' = \|Y(t_2) - Y(t_k)\| > \varepsilon$, where ε is a threshold value, $t_k = t_j + t_2 - t_1$;

Step 3 If $t_k = (n-m+1)$, go to Step 4; else let point $Y(t_k)$ be the initial point, and go to Step 2;

Step 4 Let the number iterations be N; the largest Lyapunov exponent is then

$$\hat{\lambda} = (1/(t_N - t_1))\sum_{i=1}^{N} Ln(L_i'/L_i). \tag{8}$$

in the time dimension, which can determine the horizon of system prediction. Using joint probability to describe the information of orbits in phase space,

$$K = \lim_{\tau\to 0}\lim_{\varepsilon\to 0}\lim_{n\to\infty}(n\tau)^{-1} \sum_{i_0,i_1,...,i_n}^{n} p(i_0, i_1, ..., i_n)\ln(i_0, i_1, ..., i_n)$$

where τ is the sampling time of orbit observation, ε is the unit grid size in phase space, and n is the number of phase points. Because the dynamic equations of pedestrian flow are usually unknown, there are difficulties in working with the problem $\tau \to \infty$, so we approximate the K-Entropy with Renyi entropy of order 2:

$$K_2 = \lim_{\substack{r\to 0\\ m\to\infty}} K_2(m, r)$$

and

$$K_2(m, r) = \frac{1}{\tau}\ln\frac{C(m, r)}{C(m+1, r)},$$

$$C(m, r) = \lim_{N\to\infty}\frac{1}{N^2}\sum_{i,j=1;i\neq j}^{N} H\left(r - \left\|Y(t_i) - Y(t_j)\right\|\right),$$

where N is the number of phase points in space R^m, m is the embedding dimension of the time series and denotes the Heaviside step function, and $\left\|Y(t_i) - Y(t_j)\right\|$ denotes the distance between two phase points. In the process of calculating Renyi entropy, we can obtain the correlation dimension of chaotic time series.

$$d(m, r) = LnC(m, r)/\ln r,$$

where the range of r values is [2, 600], and the unit of r is one pedestrian.

D. THE CHAOTIC CHARACTERISTICS OF PEDESTRIAN FLOWS

The time series data of pedestrian flow were collected from a Beijing CPTH during rush hours, and the time statistical interval of the time series was 1 min. These data were

collected from seven pedestrian facilities, such as passageway D1, escalator D2, staircases D3 and D4, and ticket halls D5 and D6.

The calculation of the delay time, embedding dimension and largest Lyapunov exponent are shown in Tab. 1. The results show that most pedestrian flows have chaotic characteristics except the flow on escalators. The value of the escalator was labeled with blue color in Tab. 1.

TABLE 1. Delay time τ, embedding dimension m and Lyapunov exponent λ.

	D1	D2	D3	D4	D5	D6
In	0.35	0.02	0.33	0.07	0.30	0.58
En	0.12	0.00	0.18	-0.17	0.11	0.40
τ	2	2	3	2	3	3
m	3	4	3	3	3	3
λ	0.10	-0.03	0.03	0.09	0.09	0.04

*Note. 'In' and 'En' indicate the initial and ending values of the autocorrelation function, respectively.

TABLE 2. The correlation dimension and Kolmogov entropy.

	D1	D2	D3	D4	D5	D6
τ	2	2	3	2	3	3
m	3	4	3	2	3	3
Ks	0.36	0.11	0.24	0.35	0.24	0.24

*Note. Symbol m indicates the correlation dimensions, and Ks denotes the value of K-Entropy.

The correlation dimension of the D1 data can be seen in Fig. 1. We can see the chaos attractors exist only in a limited range of nonscale intervals. When embedding dimension m is certain, the K-Entropy value will decrease with increasing r value, and we take the smallest value of the K-Entropy (see Tab. 2). The reciprocal of K-Entropy is the horizon of the system orbit prediction, so the horizons of the forecast of the short-term pedestrian flow are 3 to 5 time steps, where the sample time step is 1 min.

IV. WAVELET SUPPORT VECTOR REGRESSION

In the mass transit hub, most passenger flows have chaotic characteristics. In this section, we focus on the method of chaotic passenger flow prediction.

A. PHASE SPACE RECONSTRUCTION

Suppose there is a dataset $\{x_i, y_i; i = 1, 2, ..., N\}$, where $x_i \in R^n$ denotes the input vector and $y_i \in R$ is the output value. The idea of support vector regression is to project the data $x_i \in R^n$ into a higher-dimensional space by a kernel function Φ and classify these data with a hyperplane in the space. The linear classify function of the support vector machine was defined as

$$f(x, \omega) = \omega^T \Phi(x) + b, \tag{9}$$

The coefficients can be estimated by finding the extreme value of the function

$$R(D) = \frac{1}{2}\|\omega\|^2 + \frac{D}{l}\sum_{i=1}^{l}|y_i - f(x_i, \omega)|_\sigma, \tag{10}$$

where D is a positive constant, ε is a small positive number, and the item on the right side of Eq.(9) $|y - f(x, \omega)|_\sigma$ is set to zero when $|y - f(x, \omega)| < \sigma$ and $(|y - f(x, \omega)| - \sigma)$ when $|y - f(x, \omega)| \geq \sigma$.

Based on the Lagrange multiplier method, Eq.(8) can be written in the following form:

$$f(x) = \sum_{i=1}^{l}(\upsilon_i^* - \upsilon_i)K(x, x_i) + b, \tag{11}$$

where υ_i^* and υ_i are Lagrange multipliers, satisfying $\upsilon_i^* \times \upsilon_i = 0$, $\upsilon_i^* > 0$ and $\upsilon_i > 0$. The minimization of Eq.(10) leads to the following dual optimization form:

$$\begin{aligned}\max\ L(\upsilon_i^*, \upsilon_i) = &-\sigma\sum_{i=1}^{l}(\upsilon_i^* - \upsilon_i) + \sum_{i=1}^{l}(\upsilon_i^* - \upsilon_i)y_i \\ &- \frac{1}{2}\sum_{i=1}^{l}\sum_{j=1}^{l}(\upsilon_i^* - \upsilon_i)(\upsilon_j^* - \upsilon_j)K(x_i, x_j), \\ \text{st.}\ \sum_{i=1}^{l}(\upsilon_i^* - \upsilon_i) = 0, &\quad \upsilon_i^{(*)} \in [0, D].\end{aligned} \tag{12}$$

The kernel $K(x_i, x_j)$ form can be written in dot form $\Phi(x_i)^T\Phi(x_j)$.

B. THE WAVELET KERNEL

Let $w(x)$ be a mother wavelet function

$$w_{a,c}(x) = |a|^{-1/2}\, w\left(\frac{x - c}{a}\right), \tag{13}$$

where a is a dilation factor, and c is a translation factor. The wavelet transform of a function $f(x) \in L^2(R)$ can be written as

$$W_{a,c}(f) = \langle f(x), w_{a,c}(x)\rangle,$$

and we can reconstruct function $f(x)$ as follows:

$$f(x) = W_w^{-1}\int_0^\infty\int_{-\infty}^\infty W_{a,c}(f)w_{a,c}(x)\frac{da}{a^2}dc, \tag{14}$$

where

$$\begin{aligned}W_w &= \int_0^\infty \frac{|F(t)|^2}{|t|}dt, \\ F(t) &= \int w(x)\exp(-jtx)dx.\end{aligned}$$

The multidimensional wavelet function can be written as follows:

$$w(x) = \prod_{i=1}^{m} w(x_i), \quad x \in R^m. \tag{15}$$

Therefore, we obtain the wavelet kernels in dot-product form as follows:

$$K(x, x') = \prod_{i=1}^{m} w\left(\frac{x_i - c_i}{a}\right) w\left(\frac{x_i' - c_i'}{a}\right), \tag{16}$$

the translation invariant kernels form was $K(x, x') = K(x - x')$,

$$K(x, x') = \prod_{i=1}^{m} w\left(\frac{x_i - x_i'}{a}\right), \tag{17}$$

We construct the translation invariant kernel by the Morlet wavelet function:

$$w(x) = \cos(w_0 x)\exp(-x^2/2), \tag{18}$$

the wavelet kernel of Eq.(17) is written as follows:

$$K(x, x') = \prod_{i=1}^{m} \cos w_0 \left(\frac{x_i - x_i'}{a}\right) \cdot \exp\left(-\frac{(x_i - x_i')^2}{2a^2}\right), \tag{19}$$

Thus, we can obtain the regression function of WSVM based on Eq.(10) and (18):

$$f(x) = \sum_{i=1}^{l} (\upsilon_i - \upsilon_i^*) \prod_{j=1}^{m} \cos w_0 \left(\frac{x^j - x_i^j}{a_i}\right) \cdot \exp\left(-\frac{(x^j - x_i^j)^2}{2a_i^2}\right) + b, \tag{20}$$

where x_i^j denotes the ith training point in the jth dimension.

C. CHAOTIC TIME SERIES FORECASTING MODEL

Suppose that the length of a chaotic time series is n, and the embedding dimension and delay time are m and τ, respectively. We can reconstruct the phase space by the one-dimensional time series based on Eq.(1), with $(n - (m-1)\tau)$ points $Y(t)$ in the reconstructed phase space:

$$\begin{aligned} Y(1) &= (x(1), x(1+\tau), ..., x(1+(m-1)\tau)), \\ &... = ..., \\ Y(t) &= (x(t), x(t+\tau), ..., x(t+(m-1)\tau)), \\ &... = ..., \\ Y(M) &= (x(n-(m-1)\tau), \\ &\quad x(n-(m-1)\tau+\tau), ..., x(n)), \end{aligned} \tag{21}$$

where $M = n-(m-1)\tau$, and t is an integer where $t \in [1, M]$.

Let the phase point $Y(t)$ be the input data and the corresponding $x(t + (m-1)\tau + 1)$ in one dimension be the output data (see Eq.(19)). Chaotic motion is not random, and the Lyapunov exponent describes the divergent velocity of a pair of neighbor phase points in the system, so the trajectory of phase points is predictable in the range of critical time $(1/\lambda_{\max})$. Thus, there generally is a compound mapping

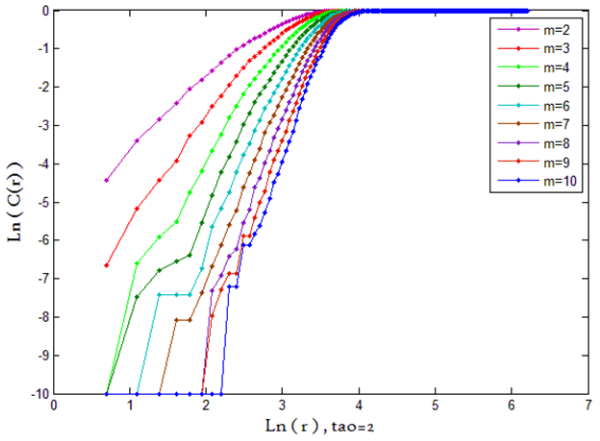

FIGURE 2. The correlation dimension of Data1.

$M'(R^m \to R^m \to R)$ among $Y(t)$, $Y(t+1)$ and $x(t + (m-1)\tau + 1)$, which is written as follows:

$$M' : Y(t) \to Y(t+1) \to x(t + (m-1)\tau + 1),$$

where compound mapping M' can be simplified in the form $M(R^m \to R)$,

$$M : Y(t) \to x(t + (m-1)\tau + 1), \tag{22}$$

Based on the training data $Y(t)$ and $x(t + (m-1)\tau + 1)$, we can use various regression methods to find the mapping M for chaotic time series forecasting.

V. EXPERIMENT RESULTS

We collected the pedestrian flow data from a Beijing CPTH during rush hours. The "*data1*" set in Tab.(1) was selected as the chaotic time series data for the experiment of regression model and forecasting. The length of the time series of data D1 was 184, with time steps of 1 min.

Four regression methods were used for modeling the mapping M of Eq.(21): the backpropagation (BP) neural network, autoregressive and moving average model (ARMA), radial basis function support vector regression model (RSVR) and the WSVR, where, the first three classical models were chose to used as baseline models In the BP neural network model, we used the hyperbolic tangent sigmoid transfer function. The hidden layer size was set to five, and the network updated its weight and bias values according to Levenberg-Marquardt optimization. We found the minimum value of Akaike's information criterion for estimating parameters p and q of the ARMA model. The index MSE was selected as a criterion for finding the optimal dilation factor a of the kernel wavelet function.

The values of last 50 steps of the time series were used to verify the regression model. The embedding dimension of "*data1*" was 3, and the delay time was 2 (see Tab. 1). We reconstructed the phase space and the set of support vector training data (see Fig.(1)). The prediction performance of the regression models was described by using statistical indices of the mean square error (MSE), the mean

TABLE 3. Mean square errors of four models on fifty time steps.

	1	2	3	4	5	6	7	8	9	10
BPNN 1	0.098999	0.13029	0.028545	0.037096	0.091225	0.16971	0.11959	0.022891	0.36665	0.14877
ARMA	0.11693	0.016716	0.1062	0.21003	0.18563	0.074712	0.045457	0.0046506	0.26647	0.27622
RSVR	0.11529	0.14768	0.10689	0.074938	0.20716	0.20716	0.19342	0.20716	0.27966	0.10953
WSVR	0.024907	0.13296	0.11943	0.047485	0.12462	0.1686	0.057302	0.032849	0.33045	0.17913
BPNN 1	0.25196	0.16114	0.014781	0.0092471	0.06519	0.34738	0.0059201	0.3025	0.13481	0.18665
ARMA	0.058875	0.075704	0.2833	0.14851	0.15594	0.23743	0.016931	0.27688	0.07231	0.15288
RSVR	0.11063	0.20977	0.074938	0.034679	0.078507	0.20025	0.12581	0.22949	0.14768	0.20025
WSVR	0.028942	0.051795	0.047167	0.0057081	0.11425	0.0014626	0.0030625	0.021525	0.038405	0.080417
BPNN 1	0.037271	0.28032	0.11282	0.17389	0.091208	0.32662	0.03258	0.47481	0.049019	0.10373
ARMA	0.036608	0.25287	0.17192	0.028092	0.040672	0.15777	0.2732	0.40228	0.089913	0.016787
RSVR	0.12581	0.37044	0.13034	0.10441	0.20716	0.20025	0.078507	0.57875	0.14768	0.10441
WSVR	0.1207	0.058394	0.019944	0.11712	0.036478	0.010181	0.07861	0.3487	0.14983	0.047824
BPNN 1	0.0087924	0.40573	0.23349	0.10566	0.068545	0.16611	0.087695	0.027972	0.25851	0.17535
ARMA	0.055983	0.25055	0.048698	0.04038	0.041311	0.39987	0.080266	0.0063603	0.14528	0.022206
RSVR	0.11063	0.11572	0.19342	0.14768	0.11063	0.1895	0.12932	0.10689	0.20977	0.19342
WSVR	0.014821	0.040037	0.066609	0.036659	0.13003	0.22889	0.14846	0.015733	0.26509	0.24912
BPNN 1	0.17282	0.05481	0.11481	0.32484	0.020605	0.0051901	0.02519	0.031595	0.068822	0.056552
ARMA	0.17503	0.023505	0.077066	0.18258	0.1982	0.067871	0.084699	0.071378	0.075877	0.0093139
RSVR	0.078507	0.10689	0.12581	0.20025	0.11529	0.13034	0.12639	0.078507	0.018255	0.11529
WSVR	0.088502	0.027646	0.068939	0.025134	0.050368	0.17609	0.11433	0.024218	0.012347	0.032823

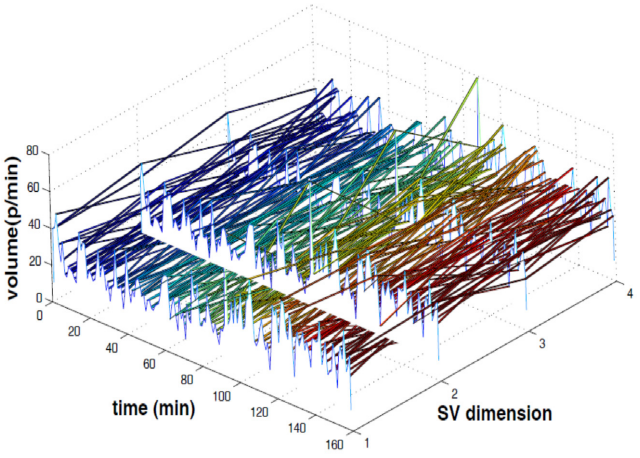

FIGURE 3. The pool of vector training samples.

TABLE 4. Total errors of four models on fifty time steps.

	BPNN	ARMA	RSVR	WSVR
MSE	8.1997	7.0023	6.8896	6.0740
MAE	6.1507	5.1597	6.4791	4.5771
MAPE	0.1753	0.1752	0.1963	0.1488

absolute error (MAE) and the mean absolute percentage error (MAPE). The results can be seen in Tab. 2.

$$MAE = n^{-1} \sum |x_i - \hat{x}_i|,$$

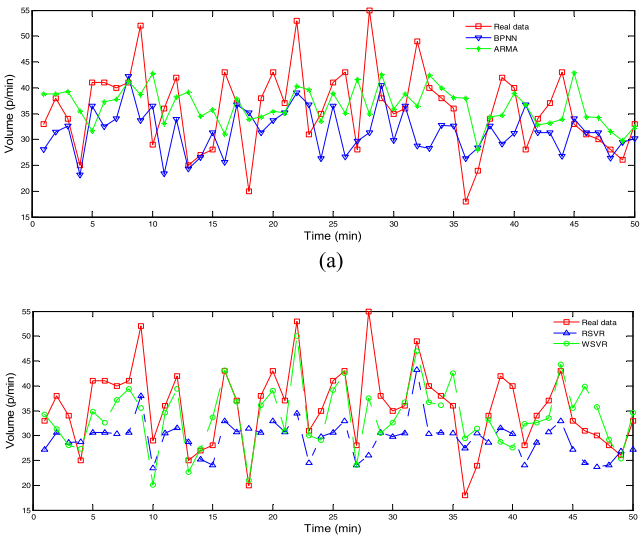

FIGURE 4. The results of regression models for forecasting. (a) Data of BP neural network and ARMA. (b) Data of RBF and Wavelet SVR model.

$$MSE = \left(n^{-1} \sum (x_i - \hat{x}_i)^2\right)^{1/2},$$
$$MAPE = n^{-1} \sum |x_i - \hat{x}_i| \cdot |x_i|^{-1}, \quad (23)$$

The performance comparison among the BPNN, ARMA, RSVR and WSVR regression models can be seen in Fig. 2 and Tab. 3. According to the values of the statistical error indices, the WSVR regression model has the lowest errors.

VI. CONCLUSIONS

In this paper, we investigated the chaotic characteristics of pedestrian flows collected from a comprehensive passenger transport hub and found that most pedestrian flows were chaotic in limited no-scale intervals, except the flows collected from escalators. Furthermore, based on the reconstruction of phase space, we used the wavelet support vector regression model to map the evolution of the trajectory in one step for chaotic time series forecasting. The results showed that the chaotic wavelet support vector regression model has better prediction accuracy. We plan to consider the random factor and fuzzy method in future work [27]–[38].

REFERENCES

[1] G. G. Løvås, "Modeling and simulation of pedestrian traffic flow," *Transp. Res. B, Methodol.*, vol. 28, no. 6, pp. 429–443, Dec. 1994.
[2] T. Ming, J. H. Fei, and J. Z. Cai, "Pedestrian agent navigation approach in virtual passenger transfer hub," in *Proc. WASE Int. Conf. Inf. Eng.*, Aug. 2010, pp. 131–135.
[3] J. Guo, W. Huang, and B. M. Williams, "Adaptive Kalman filter approach for stochastic short-term traffic flow rate prediction and uncertainty quantification," *Transp. Res. C, Emerg. Technol.*, vol. 43, pp. 50–64, Jun. 2014.
[4] D. Ma, B. Sheng, S. Jin, X. Ma, and P. Gao, "Short-term traffic flow forecasting by selecting appropriate predictions based on pattern matching," *IEEE Access*, vol. 6, pp. 75629–75638, 2018.
[5] Y. Li *et al.*, "Multiple measures-based chaotic time series for traffic flow prediction based on Bayesian theory," *Nonlinear Dyn.*, vol. 85, no. 1, pp. 179–194, Jul. 2016.
[6] I. M. Wagner-Muns, I. G. Guardiola, V. A. Samaranayke, and W. I. Kayani, "A functional data analysis approach to traffic volume forecasting," *IEEE Trans. Intell. Transp. Syst.*, vol. 19, no. 3, pp. 878–888, Mar. 2017.
[7] A. Mozo, B. Ordozgoiti, and S. Gémez-canaval, "Forecasting short-term data center network traffic load with convolutional neural networks," *PLoS ONE*, vol. 13, no. 2, Feb. 2018, Art. no. e0191939.
[8] B. Sun, W. Cheng, P. Goswami, G. Bai, "Short-term traffic forecasting using self-adjusting k-nearest neighbours," *IET Intell. Transp. Syst.*, vol. 12, no. 1, pp. 41–48, Feb. 2018.
[9] J. Guo, Z. Liu, W. Huang, Y. Wei, and J. Cao, "Short-term traffic flow prediction using fuzzy information granulation approach under different time intervals," *IET Intell. Transp. Syst.*, vol. 12, no. 2, pp. 143–150, Mar. 2018.
[10] J. Zhao, Y. Gao, Y. Qu, H. Yin, Y. Liu, and H. Sun, "Travel time prediction: Based on gated recurrent unit method and data fusion," *IEEE Access*, vol. 6, pp. 70463–70472, 2018.
[11] J. Qiao, L. Wang, C. Yang, and K. Gu, "Adaptive levenberg-marquardt algorithm based echo state network for chaotic time series prediction," *IEEE Access*, vol. 6, pp. 10720–10732, 2018.
[12] A. Wolf, J. B. Swift, H. L. Swinney, and J. A. Vastano, "Determining Lyapunov exponents from a time series," *Phys. D, Nonlinear Phenomena*, vol. 16, no. 3, pp. 285–317, Jul. 1985.
[13] M. B. Kennel, R. Brown, and H. D. I. Abarbanel, "Determining embedding dimension for phase-space reconstruction using a geometrical construction," *Phys. Rev. A, Gen. Phys.*, vol. 45, no. 6, pp. 3403–3411, Mar. 1992.
[14] S. Li, L. J. Liu, and H. L. Guo, "Comparative of the predictive method of chaos in short-term traffic flow," *Syst. Eng.*, vol. 29, no. 9, pp. 60–64, 2009.
[15] V. A. Gromov and A. N. Shulga, "Chaotic time series prediction with employment of ant colony optimization," *Expert Syst. Appl.*, vol. 39, no. 9, pp. 8474–8478, Jul. 2012.
[16] B. H. Petkov V. Vitale, M. Mazzola, C. Lanconelli, and A. Lupi, "Chaotic behaviour of the short-term variations in ozone column observed in arctic," *Commun. Nonlinear Sci. Numer. Simul.*, vol. 26, nos. 1–3, pp. 238–249, Sep. 2015.
[17] X. Sun, Y. Chen, Y. Shao, C. Li, and C. Wang, "Robust nonparallel proximal support vector machine with Lp-norm regularization," *IEEE Access*, vol. 6, pp. 20334–20347, 2018.
[18] A. J. Smola, B. Schölkopf, and K.-R. Müller, "The connection between regularization operators and support vector kernels," *Neural Netw.*, vol. 11, no. 4, pp. 637–649, Jun. 1998.
[19] W.-C. Hong, "Traffic flow forecasting by seasonal SVR with chaotic simulated annealing algorithm," *Neurocomputing*, vol. 74, nos. 12–13, pp. 2096–2107, Jun. 2011.
[20] L. Zhang, W. Zhou, and L. Jiao, "Wavelet support vector machine," *IEEE Trans. Syst., Man, Cybern. B, Cybern.*, vol. 34, no. 1, pp. 34–39, Feb. 2004.
[21] L.-B. Tang, L.-X. Tang, and H.-Y. Sheng, "Forecasting volatility based on wavelet support vector machine," *Expert Syst. Appl.*, vol. 36, no. 2, pp. 2901–2909, Mar. 2009.
[22] S. Hou, Y. Zhou, H. Liu, and N. Zh, "Wavelet support vector machine algorithm in power analysis attacks," *Radioengineering*, vol. 26, no. 3, pp. 890–902, 2017.
[23] H. Dai and Z. Cao, *A Wavelet Support Vector Machine-Based Neural Network Metamodel for Structural Reliability Assessment*. Hoboken, NJ, USA: Wiley, 2017.
[24] B. Yadav and K. Eliza, "A hybrid wavelet-support vector machine model for prediction of lake water level fluctuations using hydro-meteorological data," *Measurement*, vol. 103, pp. 294–301, Jun. 2017.
[25] H. Su, X. Li, B. Yang, and Z. Wen, "Wavelet support vector machine-based prediction model of dam deformation," *Mech. Syst. Signal Process.*, vol. 110, pp. 412–427, Sep. 2018.
[26] R.-H. Zhang, Z.-C. He, H.-W. Wang, F. You, and K.-N. Li, "Study on self-tuning tyre friction control for developing main-servo loop integrated chassis control system," *IEEE Access*, vol. 5, pp. 6649–6660, 2017.
[27] G. Tian, M. Zhou, and P. Li, "Disassembly sequence planning considering fuzzy component quality and varying operational cost," *IEEE Trans. Autom. Sci. Eng.*, vol. 15, no. 2, pp. 748–760, Apr. 2018.
[28] G. Tian *et al.*, "Operation patterns analysis of automotive components remanufacturing industry development in China," *J. Cleaner Prod.*, vol. 64, pp. 1363–1375, Oct. 2017.
[29] G. Tian, H. Zhang, Y. Feng, D. Wang, Y. Peng, and H. Jia, "Green decoration materials selection under interior environment characteristics: A grey-correlation based hybrid MCDM method," *Renew. Sustain. Energy Rev.*, vol. 81, pp. 682–692, Jan. 2018.
[30] X. J. Sun, H. Zhang, W. J. Meng, R. H. Zhang, K. L. Li, and T. Peng, "Primary resonance analysis and vibration suppression for the harmonically excited nonlinear suspension system using a pair of symmetric viscoelastic buffers," *Nonlinear Dyn.*, vol. 94, no. 2, pp. 1243–1265, Oct. 2018, doi: 10.1007/s11071-018-4421-9.
[31] H. Xiong, X. Zhu, and R. Zhang, "Energy recovery strategy numerical simulation for dual axle drive pure electric vehicle based on motor loss model and big data calculation," *Complexity*, vol. 2018, Aug. 2018, Art. no. 4071743. doi: 10.1155/2018/4071743.
[32] L. Yang, B. Wang, R. Zhang, H. Zhou, and R. Wang, "Analysis on location accuracy for the binocular stereo vision system," *IEEE Photon. J.*, vol. 10, no. 1, pp. 1–16, Feb. 2018.
[33] X. Kong *et al.*, "Mobility dataset generation for vehicular social networks based on floating car data," *IEEE Trans. Veh. Technol.*, vol. 67, no. 5, pp. 3874–3886, May 2018.
[34] A. Rahim *et al.*, "Vehicular social networks: A survey," *Pervasive Mobile Comput.*, vol. 43, pp. 96–113, Jan. 2018.
[35] X. Kong, X. Song, F. Xia, H. Guo, J. Wang, and A. Tolba, "LoTAD: Long-term traffic anomaly detection based on crowdsourced bus trajectory data," *World Wide Web*, vol. 21, no. 3, pp. 825–847, May 2018.
[36] X. Kong, M. Li, T. Tang, K. Tian, L. Moreira-Matias, and F. Xia, "Shared subway shuttle bus route planning based on transport data analytics," *IEEE Trans. Autom. Sci. Eng.*, vol. 15, no. 4, pp. 1507–1520, Oct. 2018, doi: 10.1109/TASE.2018.2865494.
[37] G. Tian, Y. Ren, Y. Feng, M. Zhou, H. Zhang, and J. Tan, "Modeling and planning for dual-objective selective disassembly using AND/OR graph and discrete artificial bee colony," *IEEE Trans. Ind. Informat.*, 2018, doi: 10.1109/TII.2018.2884845.
[38] T. Nguyen, I. Hettiarachchi, A. Khatami, L. Gordon-Brown, C. Lim, and S. Nahavandi, "Classification of multi-class BCI data by common spatial pattern and fuzzy system," *IEEE Access*, vol. 6, pp. 7873–27884, 2018.

MING TANG received the B.S. and M.S. degrees in transportation engineering from the Changsha University of Science and Technology, Changsha, China, in 1999 and 2004, respectively, and the Ph.D. degree from Jilin University, Changchun, China, in 2010, where he is currently an Instructor of the Transportation College. His research interests include intelligent transportation and slow traffic system planning.

ZHIWU LI (M'06–SM'07–F'16) received the B.S. degree in mechanical engineering, the M.S. degree in automatic control, and the Ph.D. degree in manufacturing engineering from Xidian University, Xi'an, China, in 1989, 1992, and 1995, respectively. In 1992, he joined Xidian University. He was a Visiting Professor with the University of Toronto, Technion (Israel Institute of Technology), Martin-Luther University, Conservatoire National des Arts et Métiers, Meliksah Universitesi, King Saud University, and the University of Cagliari. He is currently with the Institute of Systems Engineering, Macau University of Science and Technology, Macau. His current research interests include Petri net theory and application, supervisory control of discrete event systems, work flow modeling and analysis, system reconguration, game theory, and data and process mining.

He is a member of the Discrete Event Systems Technical Committee of the IEEE Systems, Man, and Cybernetics Society, and the IFAC Technical Committee on Discrete Event and Hybrid Systems, from 2011 to 2014. He is listed in Marquis Who's Who in the World, 27th Edition, in 2010. He received the Alexander von Humboldt Research Grant from the Alexander von Humboldt Foundation, Germany, and Research in Paris, France. He is the Founding Chair of the Xi'an Chapter of the IEEE Systems, Man, and Cybernetics Society. He serves as a frequent Reviewer for over 60 international journals, including *Automatica*, and a number of the IEEE TRANSACTIONS as well as many international conferences.

GUANGDONG TIAN received the B.S. degree in vehicle engineering from the Shandong University of Technology, Zibo, China, in 2007, and the M.S. and Ph.D. degrees in automobile application engineering from Jilin University, Changchun, China, in 2009 and 2012, respectively.

He is currently a Professor with the School of Mechanical Engineering, Shandong University, China. His research focuses on remanufacturing and green manufacturing, green logistics and transportation, intelligent inspection and repair of automotive, decision making, and intelligent optimization. He has published over 100 journal and conference proceedings papers in the above research areas, including the IEEE TRANSACTIONS ON AUTOMATION SCIENCE AND ENGINEERING, the IEEE TRANSACTIONS ON CYBERNETICS, and the IEEE/ACM TRANSACTIONS ON COMPUTATIONAL BIOLOGY AND BIOINFORMATICS. He is listed in Marquis Who's Who in the World, 30th Edition, in 2013. He is invited to organize several conferences and service the Session Chair, e.g., ICNAAM 2012 and ICAMechS 2015. He is a Founding Member of Sustainable Production and Service Automation of the IEEE Robotics and Automation Society. He serves as a frequent Reviewer for more than 30 international journals, including the IEEE TRANSACTIONS ON AUTOMATION SCIENCE AND ENGINEERING, the IEEE TRANSACTIONS ON SYSTEMS, MAN, AND CYBERNETICS–PART A, and the *Asian Journal of Control*.